Pergamon

PII: S0191–8141(98)00021–2

Journal of Structural Geology, Vol. 20, No. 7, pp. 945 to 955, 1998

0191-8141/98 $19.00 + 0.00

Ultra high-temperature and subsolidus shear zones: examples from the Poe Mountain anorthosite, Wyoming

BRUNO LAFRANCE,* BARBARA E. JOHN and B. RONALD FROST

Department of Geology and Geophysics, University of Wyoming, P.O. Box 3006, Laramie, WY 82071-3006, U.S.A.

(*Received* 28 *April* 1997; *accepted in revised form* 21 *January* 1998)

Abstract—Ultra high-temperature shear zones formed with interstitial melts present during the emplacement of the Poe Mountain anorthosite, Wyoming. The shear zones are characterized by coarse-grained plagioclase with flat extinction and rare deformation microstructures. Dissected grain microstructures suggest that plagioclase underwent recrystallization by 'fast' grain boundary migration. Orthopyroxene crystallized from interstitial melts as strain-free, foliation-parallel tablet grains.

Plagioclase has a magmatic petrofabric, characterized by poles to (010) normal to the shear foliation, and [100] parallel to the foliation and movement direction. Poles to (001) have a broad distribution with a point maximum roughly parallel to the foliation and normal to the movement direction. Orthopyroxene petrofabrics result from oriented growth parallel to the shear foliation. [100] defines a point maximum perpendicular to the shear foliation, and [010] and [001] have great circle distributions approximately parallel to the shear foliation.

Microstructures of the ultra high-temperature shear zones contrast with those of granulite-grade shear zones cutting across the intrusion. The granulite-grade shear zones initiated as fractures, which evolved into shear zones by dynamic recrystallization. Deformed primary plagioclase and orthopyroxene recrystallized by grain boundary rotation into smaller polygonal grains. © 1998 Elsevier Science Ltd. All rights reserved

INTRODUCTION

Shear zones are commonly associated with the emplacement and cooling of plutons. Syn-emplacement shear zones are observed along the margins of plutons intruded in active regional fault systems (Vernon *et al.*, 1989; Tobisch *et al.*, 1993), in the interior of plutons as products of the injection of new batches of magma in expanding or ballooning plutons (John and Blundy, 1993), or due to thermal contraction during cooling of the plutons (John and Blundy, 1993). Thus, shear zones form at all stages of the emplacement, growth, and cooling of plutons under a wide spectrum of magmatic to subsolidus conditions.

Ultra high-temperature shear zones formed during the emplacement and cooling of the Poe Mountain anorthosite, Wyoming (Fig. 1). The shear zones formed with interstitial melt present, with minor deformation and recrystallization continuing during cooling of the body to temperatures of 865–940°C, that is 110–185°C below the solidus temperature (1050°C) of the Poe Mountain anorthosite (Scoates, 1994). Subsolidus shear zones formed at granulite-grade conditions without melt present. We discuss and compare microstructures, recrystallization processes, and petrofabrics in the ultra-high temperature and subsolidus shear zones. The subsolidus shear zone initiated as fractures and, thus, demonstrates the importance of brittle processes, even under granulite-grade conditions.

FIELD SETTING

The Poe Mountain anorthosite (Fig. 1) is one of three large anorthosite bodies in the 1.43 Ga unmetamorphosed Laramie anorthosite complex (Scoates, 1994). The complex is surrounded by a contact metamorphic aureole, which record emplacement depths of 300 MPa (Fuhrman *et al.*, 1988; Grant and Frost, 1990). The Poe Mountain anorthosite comprises an outer zone, from 1 to 4 km wide, of well-layered anorthositic cumulates, and an inner, 8 km-wide, core of massive anorthosites, which have been pervasively recrystallized during the emplacement of the intrusion (Frost *et al.*, 1993; Scoates, 1994). Major and trace element geochemistry indicate that the Poe Mountain anorthosite is a composite body, the product of repeated injections of distinct magma batches (Scoates, 1994). The intrusion is truncated by late clay- and carbonate-rich brittle faults, which removed its eastern half. These late faults formed during the Laramide orogeny, between 1.3 and 1.4 Ga after the emplacement of the anorthosite.

Narrow shear zones occur throughout the intrusion, where they cut magmatic layering at high-angle. The subsolidus granulite-grade shear zones appear as rusty discrete faults on outcrop. The ultra high-temperature shear zones are expressed as cm-scale ductile shear

*Present address: Saskatchewan Energy & Mines, P.O. Box 5000, La Ronge, Saskatchewan, Canada S0J 1L0.

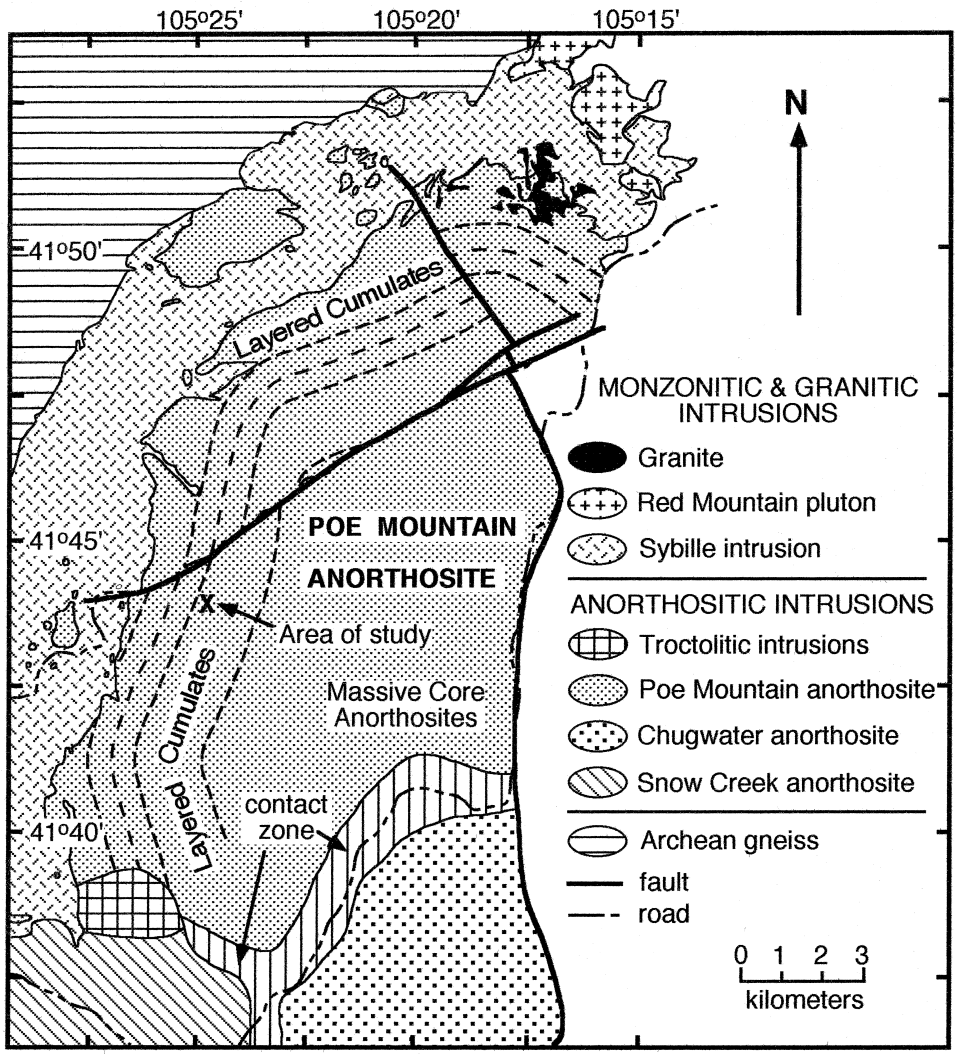

Fig. 1. Simplified geological map of the Poe Mountain anorthosite, Wyoming (after Scoates, 1994). 'X' (Lat 41°43′56″N Long 105°24′44″W) marks the location of the shear zone in Fig. 2.

zones in which primary layering was dragged and rotated into parallelism with the margins of the shear zones. The rotation occurs together with thinning of the layering and grain-size attenuation of both pyroxene and plagioclase. The microstructures discussed in the paper are from two drill core samples collected in the center of the shear zone shown in Fig. 2. The shear zone is up to 10 cm wide and narrows along strike to a discrete fault. No lineation is observed in the shear zone, but drag of the primary layering into the shear zone suggests a component of horizontal sinistral movement. Sinistral offset of layering is also observed along other parallel shear zones.

Several lines of evidence suggest that the shear zone formed at ultra high-temperature. An undeformed intrusion of megacrystic leucogabbro containing fragments of anorthosite occupies the center of the shear zone (Fig. 2a). Where the shear zone becomes a discrete fault in the upper portion of Fig. 2, the leucogabbro narrows to a 1–2 cm wide dike which follows the fault for a distance of 40 cm. The shear zone therefore formed before the last pulse of anorthositic magma was emplaced during the build-up of the anorthosite body. The leucogabbro does not contain any hydrous primary minerals; its coarse grain size (3–5 mm in diameter) implies that the anorthosite and shear zone were still very hot during the intrusion of the megacrystic leucogabbro.

MICROSTRUCTURES

Primary anorthosite and leucogabbro

Primary anorthosite and leucogabbro layers contain mainly plagioclase (An_{40-50}) with less than 35% orthopyroxene–inverted pigeonite–clinopyroxene–olivine–Fe–Ti oxides with accessory apatite, alkali feldspar and biotite. Inverted pigeonite has planar internal exsolutions of clinopyroxene and rounded exsolutions of clinopyroxene rimming the margins of orthopyroxene. The ferromagnesian minerals have equigranular,

anhedral grain shapes and generally flat extinction. The Fe–Ti oxides crystallized as oikocrysts; that is, single large poikilitic grains enclosing plagioclase.

The primary anorthosite and leucogabbro layers are porphyroclastic (Fig. 3a) to granoblastic with large porphyroclasts of plagioclase (1–2 cm grain size) surrounded by finer-grained recrystallized plagioclase (0.7 mm). Some of the large porphyroclasts have irregular amoeboidal shapes. Rare spatially separated plagioclase grains show identical optical extinction,

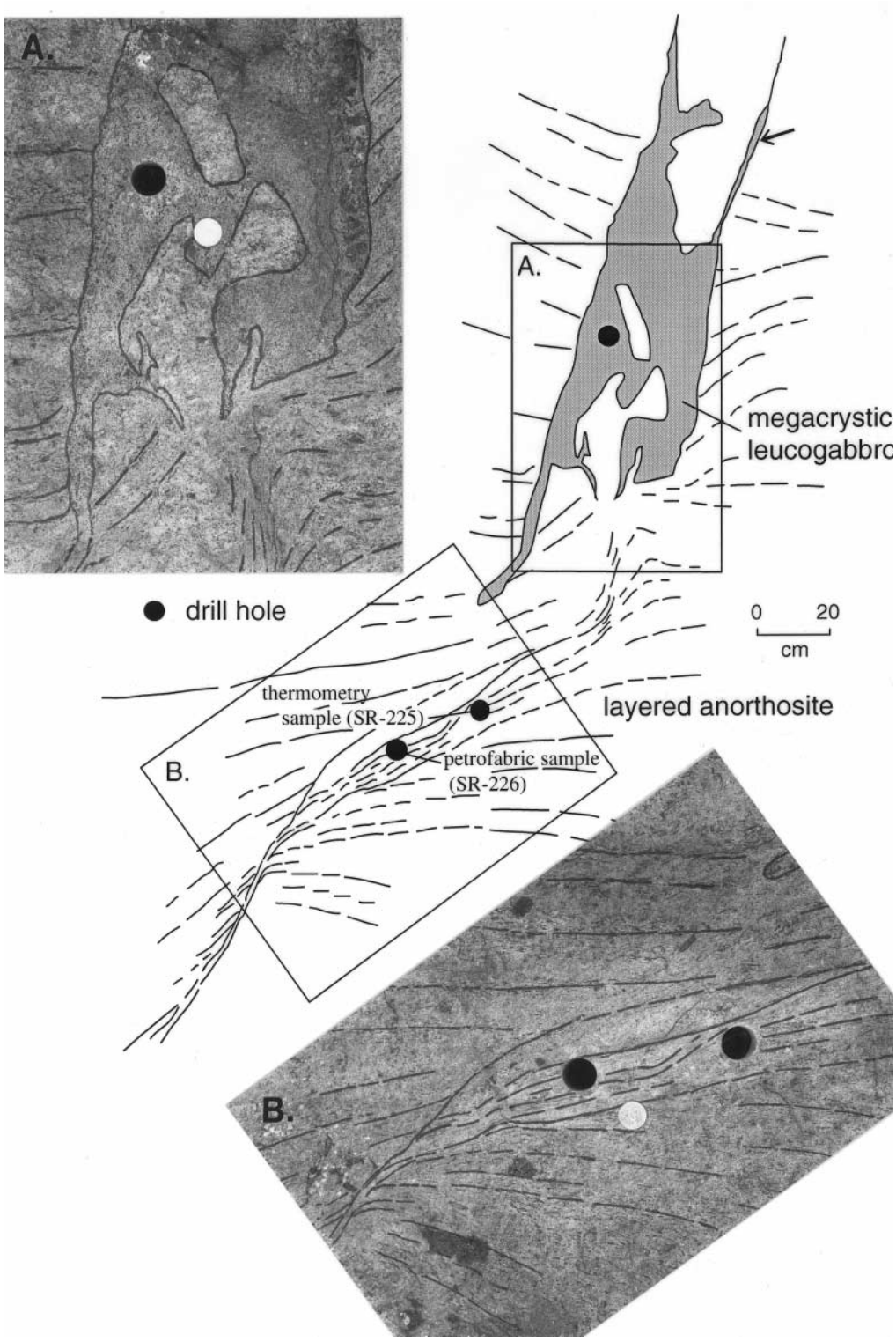

Fig. 2. Line diagram of ultra high-temperature shear zone with photographs of two areas within it. Foliations are in the shear zone and in the primary layered anorthosite and leucogabbro. Foliations in photographs have been highlighted with black marker. The shear zone becomes a fault in the upper section of the line diagram. Arrow points to a narrow leucogabbro dike intruding the fault.

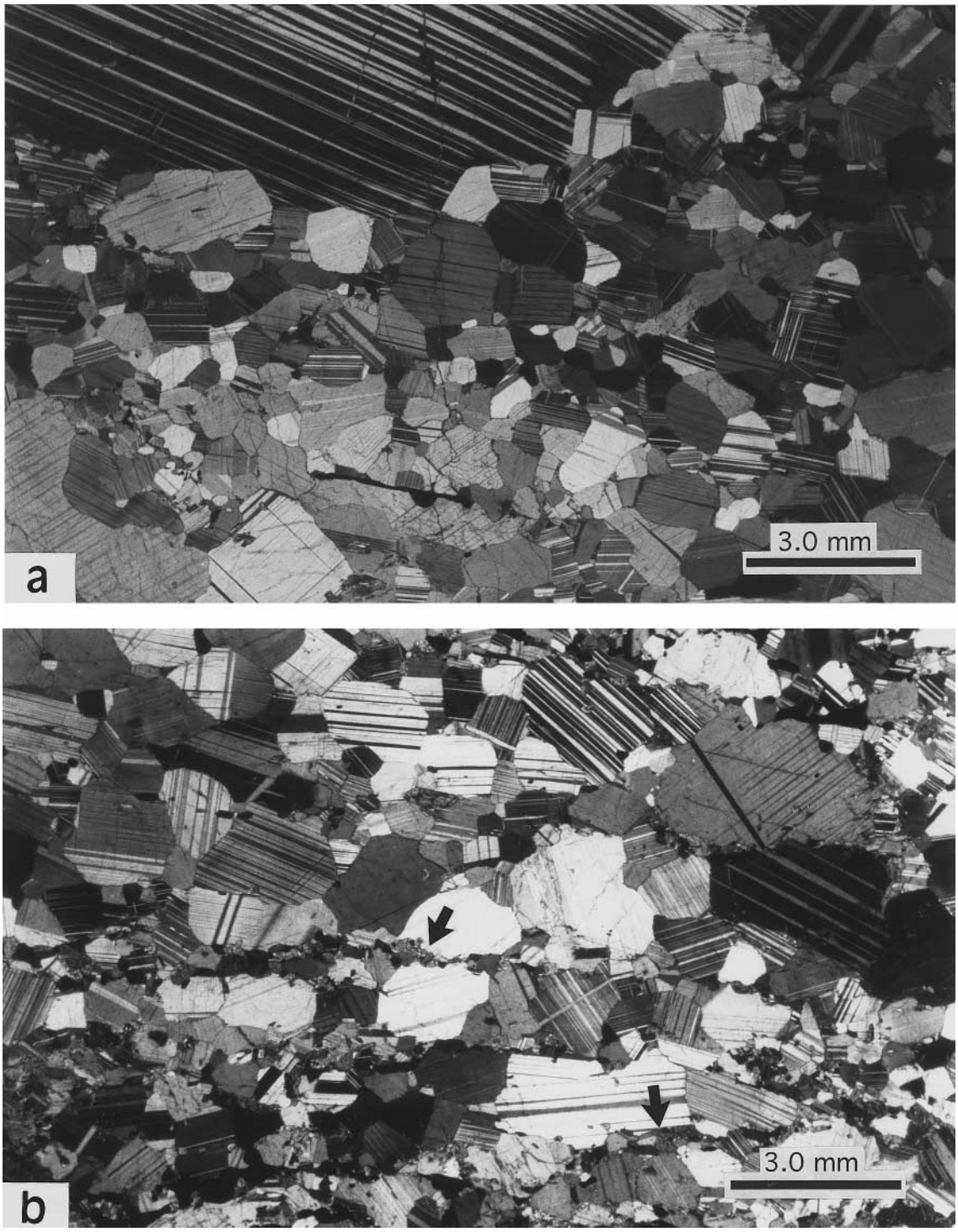

Fig. 3. (a) Photomicrograph of the porphyroclastic primary anorthosite. A large plagioclase porphyroclast in the upper section of the photomicrograph is completely surrounded by smaller recrystallized grains. (b) Photomicrograph of the ultra high-temperature shear zone. Arrows point to shear foliation defined by small grains of orthopyroxene, Fe–Ti oxides, olivine, and clinopyroxene. The section is cut perpendicular to the foliation at a high angle to the movement direction.

suggesting that they are products of the dissection of larger plagioclase grains by 'fast' grain boundary migration at very high temperatures (Lafrance *et al.*, 1996). Evidence of plastic deformation is rare and limited to a few grains having undulose extinction, low-angle boundaries, deformation twins and kink bands. Under the petrological microscope, insertion of an auxiliary gypsum plate shows a weak crystallographic preferred orientation (CPO) for plagioclase.

Ultra high-temperature shear zone

A reduction in grain size of plagioclase, Fe–Ti oxides, and ferromagnesian minerals occurs within the

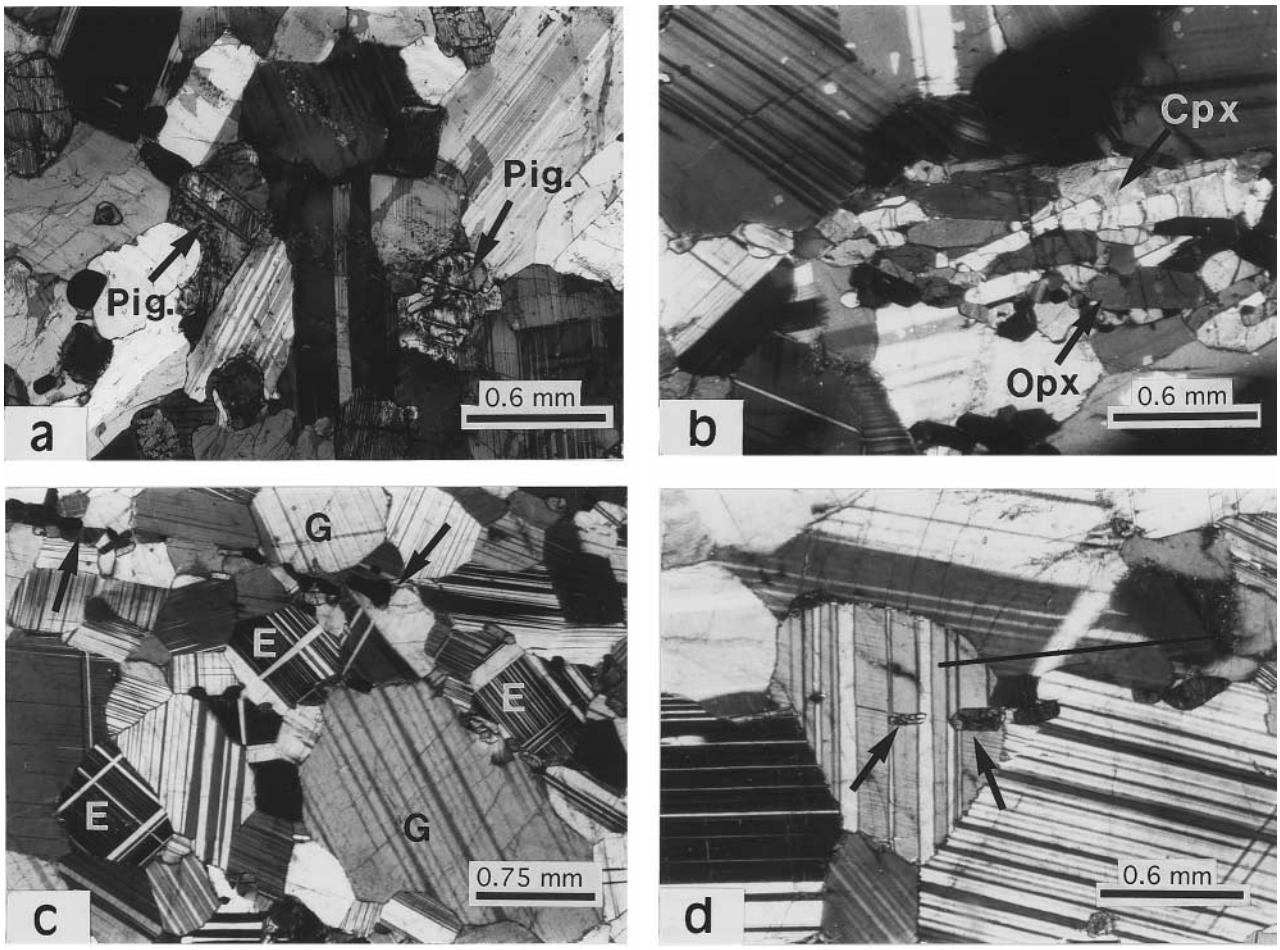

Fig. 4. Photomicrographs of microstructures in (a) primary anorthosite and (b–d) ultra high-temperature shear zone. (a) Inverted pigeonite (Pig.) with exsolutions of clinopyroxene. (b) Tabular orthopyroxene (Opx) with interstitial clinopyroxene (Cpx) define the shear foliation. Orthopyroxene is elongate parallel to the shear foliation. (c) Dissected grain microstructures in plagioclase. Grains G and E have been dissected into two and three smaller grains, respectively, by the growth of adjacent grains. Grain G is cut by shear foliation shown by arrows. (d) Tabular orthopyroxene grains shown by arrows are enclosed within a single plagioclase grain. The orthopyroxene grains are aligned parallel to the shear foliation, represented by the black line.

shear zone. The foliation in the shear zone comprises 1–2 mm wide layers of plagioclase, alternating with discontinuous, 0.25–0.5 mm wide layers of ferromagnesian minerals, Fe–Ti oxides, and apatite (Fig. 3b). The latter layers are commonly defined by isolated grains aligned along planar plagioclase grain boundaries. Primary orthopyroxene and inverted pigeonite (Fig. 4a) are replaced by smaller isolated grains and clusters of anhedral and tablet orthopyroxene grains (0.1 mm grain size) with interstitial clinopyroxene (Fig. 4b). Tabular, tablet orthopyroxene grains are elongate parallel to the shear zone foliation. Optical extinction is commonly parallel, but is also oblique to the length of the tablets. The tablet grains are strain-free, with well developed 120° triple junctions. They have long straight faces, suggesting that these grain boundaries correspond to crystallographic orientations. A few, larger, strain-free orthopyroxene grains, which vary in length from 2 to 3 mm and in width from 0.3 to 0.5 mm, are elongate parallel to the foliation. They have irregular grain boundaries, and are associated with non-contiguous, anhedral, smaller grains, having similar orientation as the larger grains. Grain boundary migration, either driven by strain energy or surface energy, probably isolated the smaller grains from their larger parent grains. Fe–Ti oxides, which originally crystallized as large oikocrysts, occur as small rounded grains fringing plagioclase grain boundaries.

Rare, deformed plagioclase grains have plastic deformation microstructures restricted to narrow deformation twins, to low-angle boundaries spanning the width of the grains, and to slight undulose extinction. The grains generally have flat extinction, grain boundary dihedral angles of 120°, and an average grain size of 0.4–0.5 mm. Although plagioclase tends to develop a granoblastic microstructure, dissected plagioclase microstructures suggest that grain boundaries were very mobile during deformation (Fig. 4c). Grain boundary migration produced 'left-over' recrystallized grains (Urai *et al.*, 1986) as larger grains were dissected into several smaller new grains due to the growth of adjacent grains. Although the microstructure may

result from syn-emplacement recrystallization of the primary layers prior to shearing (Lafrance *et al.*, 1996), foliation-parallel trails of Fe–Ti oxides, ferromagnesian minerals, and apatite are completely enclosed within single plagioclase grains, suggesting that grain boundaries were also very mobile during shearing (Fig. 4d). Rare subgrains in larger primary plagioclase are bounded by both low-angle boundaries and the grain boundaries of their host, suggesting that new plagioclase grains may have formed by increased misorientation or rotation of low-angle boundaries into high-angle boundaries (grain boundary rotation recrystallization).

Subsolidus shear zone

Millimeter-wide shear zones appear as thin recrystallized fine-grained zones in thin section. A fracture-like shear zone cuts across coarse-grained primary plagioclase, olivine, orthopyroxene coronas around olivine, biotite, and Fe–Ti oxides in Fig. 5(a). The shear zone is only 2 mm wide, and is defined by small polygonal recrystallized grains of plagioclase, orthopyroxene, and olivine. The shear zone ends as a discrete intragranular fracture in a large plagioclase megacryst. The host plagioclase has uneven extinction and is deformed against the fracture. Subgrains and new grains of similar sizes (0.05–0.10 mm) and orientations are observed in plagioclase along the fracture (Fig. 5b), implying that the shear zone initiated as a fracture which evolved into a shear zone with recrystallization. The subgrains are bounded by both high-angle and low-angle boundaries. The new grains formed by the progressive misorientation or rotation of low-angle boundaries into high-angle boundaries. In other plagioclase megacrysts, there is a transition from healed microfractures decorated with impurities and oriented parallel to the margins of the shear zone, to recrystallized microfractures, and to thin recrystallized zones of polygonal plagioclase (Fig. 5c), supporting the above interpretation.

The recrystallization of orthopyroxene into stable polygonal grains (Fig. 5d) indicates at least granulite-

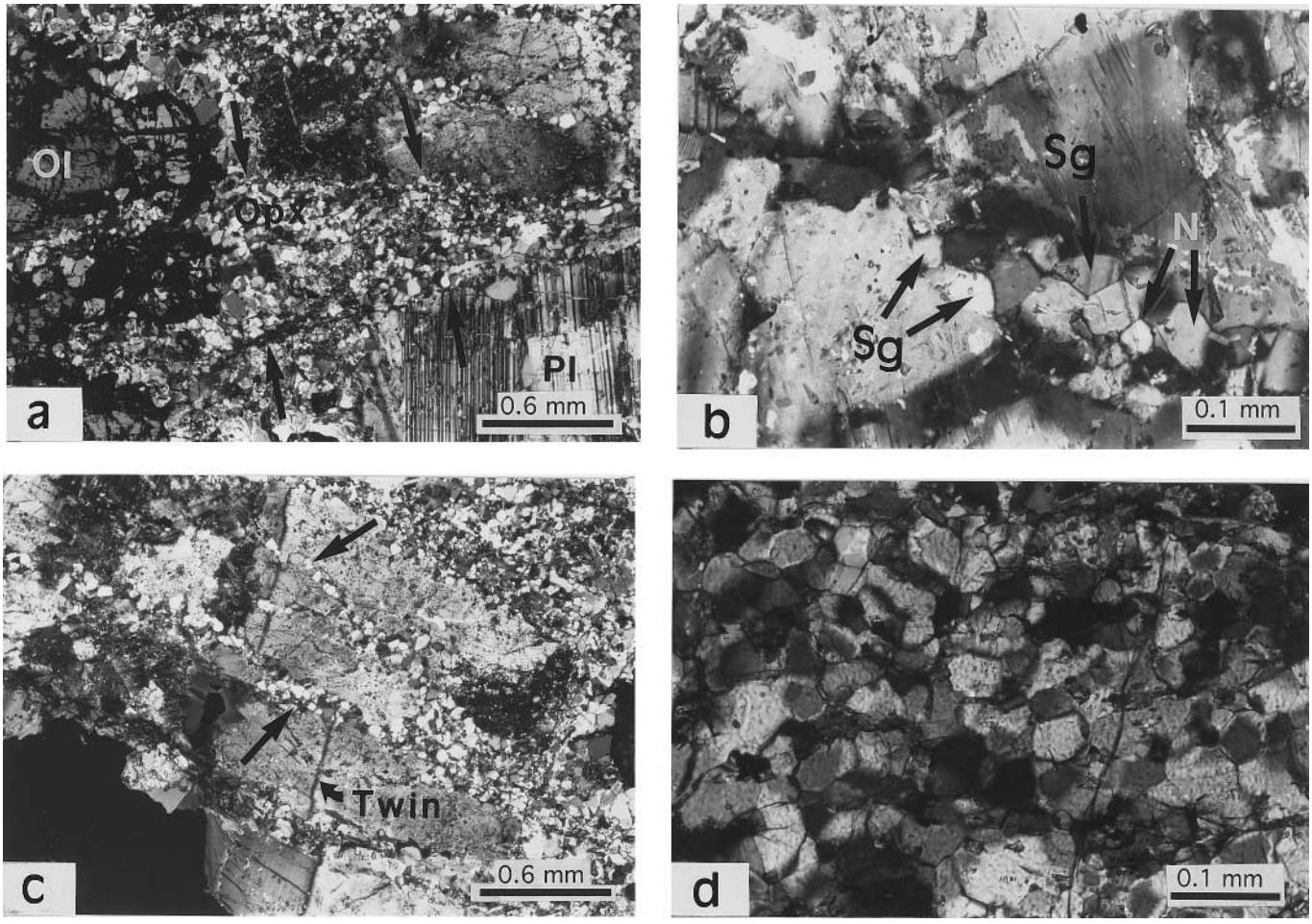

Fig. 5. Photomicrographs of microstructures in granulite-grade, subsolidus shear zone. (a) The margins of the shear zone are outlined by arrows. The shear zone cuts across primary olivine (Ol), an orthopyroxene corona around olivine, and plagioclase (Pl). The orthopyroxene corona recrystallized into smaller grains (Opx) within the shear zone. (b) Subgrains (Sg) and new grains (N) along intragranular fracture in plagioclase. The subgrains and new grains have similar sizes and orientations, implying that the new grains formed by the progressive misorientation or rotation of low-angle boundaries into high-angle boundaries. (c) A twin boundary (Twin) is displaced by several recrystallized fractures or microfaults, shown by arrows. (d) Polygonal recrystallized orthopyroxene in shear zone.

facies temperatures during deformation. The presence of low-angle boundaries dividing orthopyroxenes into subgrains bounded by both low-angle and high-angle boundaries, suggest that the new grains formed by a mechanism similar to that of plagioclase. As far as we are aware, extensive recrystallization of orthopyroxene has only been observed in granulite-grade shear zones (e.g. Giles Complex; Etheridge, 1975; Balhaus and Berry, 1991) and mantle peridotites (Bouillier and Nicolas, 1975; Drury and van Roermund, 1989; Suhr, 1993). Even at temperatures as high as 1000°C in a peridotite massif, orthopyroxene was not recrystallized and behaved as a rotating competent object in a more ductile olivine matrix (Skrotzki *et al.*, 1990); therefore, these shear zones must have formed during the emplacement and cooling of the intrusion, as the anorthosite is otherwise unmetamorphosed (Scoates, 1994).

THERMOMETRY

The fine-grained augite, hypersthene, and olivine from the ultra-high temperature shear zone have ranges of composition that are produced by ion exchange during cooling (Fig. 6). Individual spot analyses of augite form an array that trends toward lower iron with increasing Ca ($Wo_{37}En_{39}Fs_{23}$ to $Wo_{40}En_{40}Fs_{20}$), hypersthene forms a smaller field that has a subtle trend toward lower iron with decreasing Ca ($Wo_{2.3}En_{50.6}Fs_{47.1}$ to $Wo_{1.6}En_{51.6}Fs_{46.8}$). Olivine also shows a moderate range in composition (Fa_{65}–Fa_{67}). The ranges in composition are what one would expect to have formed during retrograde ion exchange, with olivine becoming more iron-rich on cooling and augite gaining Ca from hypersthene.

From the pyroxene thermometer in the QUILF program (Anderson *et al.*, 1993), we can specify three temperatures in this re-equilibration process. The lowest temperature (770 ± 40°C) is obtained from the most calcic augite and the least calcic hypersthene. The large uncertainty in this temperature reflects the fact that these pyroxenes are not in Fe–Mg exchange equilibrium. The highest temperature (865 ± 15°C) is obtained from the least calcic augite and the most calcic hypersthene. The small uncertainty in this calculated temperature indicates that these pyroxenes are nearly in Fe–Mg exchange equilibrium. However, the olivine that is in equilibrium with this pair (*ca* Fa_{60}) is far more magnesian than the olivine found in the rock. The highest temperature (*ca* 940°C) for the assemblage olivine–hypersthene–augite is determined by the lowest temperature that pigeonite would be in equilibrium with the pyroxenes of these Fe/Mg ratios. From these results we conclude that the ultra-high temperature shear zone formed at temperatures of at least ≈865°C and 940°C. The pyroxene continued to re-equilibrate by Ca and Fe–Mg exchange down to temperatures as low as 770°C, and Fe–Mg exchange between pyroxene and olivine continued down to temperatures of 500°C or lower.

The granulite-grade shear zone, unfortunately, does not contain clinopyroxene. Although we cannot get a well constrained temperature from this rock, we can use the hypersthene composition to determine the minimum temperature of formation for this shear zone. The hypersthene has the average composition of $En_{55.0}Wo_{1.5}Fs_{43.5}$. If these hypersthene grains were in equilibrium with augite they would have formed at 766 ± 30°C, where the range in temperature reflects the range in Ca content of the hypersthene. Technically, this is a minimum temperature, as augite is not found in the shear zone. However, we consider it to be a reasonable estimate for the temperature of the shear zone, since it is quite likely that the hypersthene in the shear zone (which is only millimeters wide) was in exchange equilibrium with augite elsewhere in the system, for otherwise there would be no sink for the Ca that is released from the high-T hypersthene during cooling.

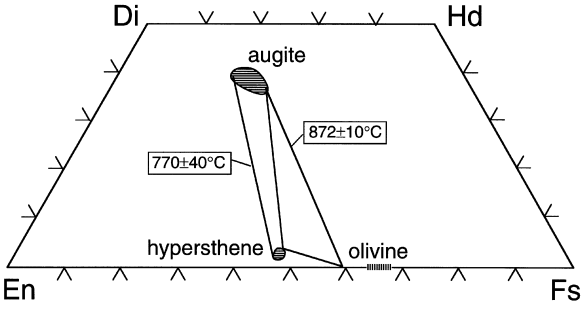

Fig. 6. Pyroxene quadrilateral showing the compositional range for pyroxenes from the ultra high-temperature shear zone. Temperatures calculated from the QUILF program (Anderson *et al.*, 1993) are given for the lowest temperature pyroxene pair and for the highest temperature pair. Note that the olivine in equilibrium with the high-temperature pyroxene pair is much more magnesian than the olivine found in the rock, indicating that Fe–Mg exchange continued to temperatures well below 770°C.

PETROFABRICS

Description of petrofabrics

Petrofabrics of plagioclase and orthopyroxene were measured on one 3-cm diameter drill core sample (SR226) from the ultra high-temperature shear zone (Fig. 2b) in an effort to document the processes operative in the shear zone (Fig. 7). Three mutually perpendicular thin sections were cut from this core sample. Measurements made on these thin sections were subsequently rotated, and are reported on a plane perpendicular to the foliation and with the movement direction horizontal.

[100], poles to (001), and poles to (010) in plagioclase grains were determined from universal stage

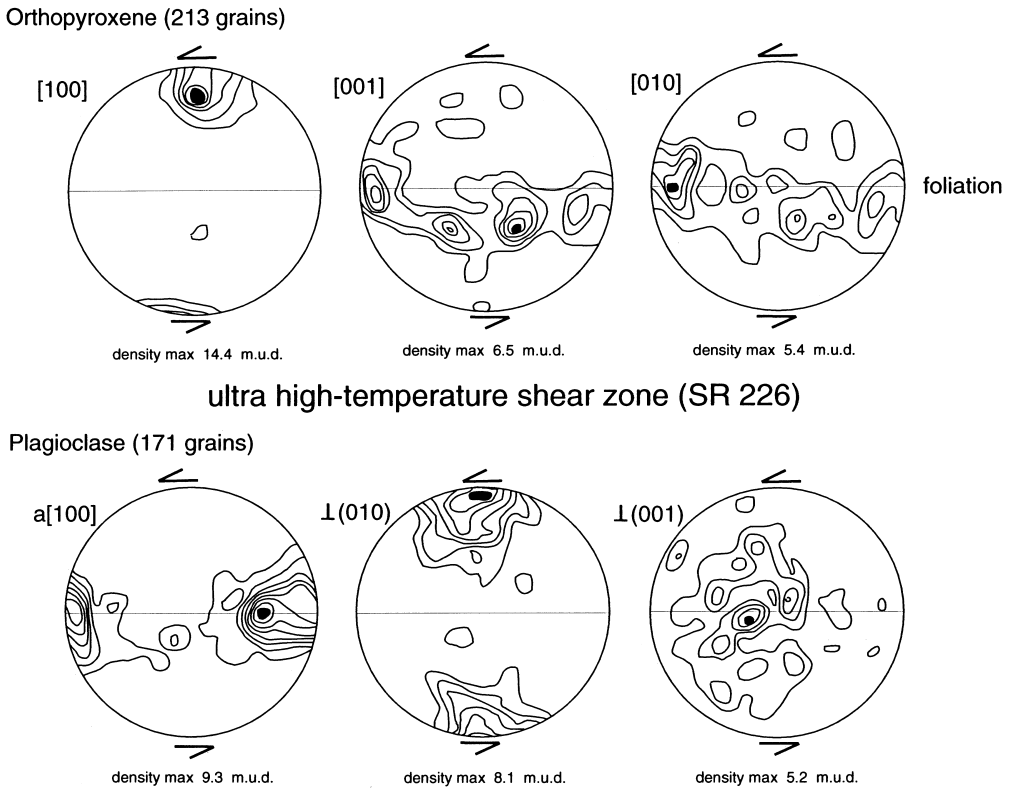

Fig. 7. Petrofabrics of orthopyroxene and plagioclase in the ultra high-temperature shear zone. Foliation is represented by E–W line; movement direction is horizontal. Equal-area lower-hemisphere projections. Contours are in double multiples of uniform distribution (m.u.d.) for the orthopyroxene [100] petrofabric and in single multiple of uniform distribution for the other petrofabrics.

measurements of the optical indicatrix, albite twin planes, and pericline twin planes, using the computer program of Benn and Mainprice (1989). Universal stage measurements were made on a total of 171 grains along five traverses across one thin section. The orientation of both pericline and albite twins were measured where possible (33% of the grains), although only one twin measurement is necessary to calculate the orientation of crystallographic directions in plagioclases with An_{40-50} composition. Ninety-six percent of the grains were measurable, thus the petrofabric is considered to be representative of the sample and shear zone, although all measurements are from only one thin section (Ji and Mainprice, 1988; Ji *et al.*, 1994).

Plagioclase in the ultra high-temperature shear zone has simple petrofabrics (Fig. 7). Poles to (010) define a point maximum perpendicular to foliation. [100] lies within the foliation and defines an elongate point maximum parallel to the movement direction. Poles to (001) have a broad distribution with a point maximum lying within the plane of the foliation at a high angle to the movement direction.

In addition, orthopyroxene has a simple petrofabric in the ultra high-temperature shear zone (Fig. 7). [100], [010], and [001] were measured on 213 orthopyroxene grains from the three mutually perpendicular thin sections. [100] defines a strong point maximum approximately perpendicular to the foliation. [010] and [001] lie approximately parallel to the foliation, and both have great circle distributions with two point maxima oriented parallel to the movement direction, and at an angle of 60–70° to the movement direction.

Interpretation of petrofabrics

The ultra high-temperature shear zone has distinctive petrofabrics. CPO of orthopyroxene has been attributed to viscous magmatic flow (Schmidt, 1952; Moore, 1973), to rigid body rotation of the orthopyroxene grains in a more ductile olivine matrix (Skrotzki *et al.*, 1990), to melt impregnation in a high-temperature deformed dunite (Suhr, 1993), and to plastic deformation (Nicolas *et al.*, 1973; Etheridge, 1975; Christensen and Lundquist, 1982; Mainprice and Silver, 1993). However, only plastic deformation produces a [100] point maximum perpendicular to the foliation, as measured in the ultra high-temperature shear zone. (001)[001] is the dominant slip system in orthopyroxene (Raleigh *et al.*, 1971). As a result of plastic deformation and recrystallization, (100) and [001] are preferentially oriented parallel to the foliation and lineation, respectively (Etheridge, 1975; Christensen and Lundquist, 1982; Mainprice and Silver, 1993). Alternatively, the petrofabrics may result from the crystallization and growth of foliation-parallel tablet orthopyroxene, producing a [100] point maximum per-

pendicular to the foliation. This interpretation is preferred, because it is consistent with the microstructure of the shear zone, discussed in the next section.

Plagioclase petrofabrics can also result either from plastic or magmatic deformation. Because (010) [001] is the dominant slip system in plagioclase (Carter and Raleigh, 1969), plastic deformation of plagioclase generally results in petrofabrics with (010) parallel to the foliation, [001] parallel to the lineation, and [100] perpendicular to both the lineation and foliation (Olsen and Kohlstedt, 1985; Olesen, 1987; Kruhl, 1987; Ji and Mainprice, 1988; Zhao *et al*., 1995). At higher temperatures and/or in plagioclase with greater An content, (001) slip parallel to the *a*-axis results in petrofabrics with (001) and [100] parallel to the foliation and lineation, respectively (Kruhl, 1987; X. O. Zhao, personal communication). The petrofabric of the ultra high-temperature shear zone has poles to (010) that define a point maximum perpendicular to the foliation and [100] clusters close to the movement direction. This fabric is different than the two types of plastic deformation petrofabrics discussed, but is similar to magmatic petrofabrics described by Benn and Allard (1989). We infer that the petrofabric of plagioclase in the ultra high-temperature shear zone is magmatic in origin. Although plagioclase contains few deformation microstructures, intracrystalline slip may still have contributed to the development of the petrofabric, because microstructures are rapidly annealed at very high temperatures, eliminating evidence of intracrystalline slip. Recrystallization may also have affected the petrofabrics. Plagioclase underwent extensive recrystallization by grain boundary migration, a process known to modify petrofabrics (Urai *et al*., 1986).

DISCUSSION

Ultra high-temperature shear zones are characterized by coarse plagioclase with flat extinction, few deformation microstructures, and dissected grain microstructures. Dissected grain microstructures are indicative of recrystallization by 'fast' grain boundary migration at very high temperatures (Regime 3 creep of Hirth and Tullis, 1992). In the layered anorthosite, recrystallization by 'fast' grain boundary migration began with interstitial melt present before complete solidification of the Poe Mountain anorthosite (Lafrance *et al*., 1996). Similar microstructures are reported in dunite and olivine deformed within melt-lubricated shear zone in the Josephine peridotite, SW Oregon (Kelemen and Dick, 1995). Dissected grain microstructures were also observed in deformation experiments on salt and analog material at $T \geq 0.7$ melting temperatures (Means, 1983; Urai, 1983; Tungatt and Humphreys, 1984), and on analog material deformed with melt present (Park and Means, 1996). Thus, dissected grain microstructures suggest that plagioclase in the ultra high-temperature shear zone recrystallized at very high temperatures, possibly in the presence of interstitial melt.

Neoblasts in deformed orthopyroxene generally adopt anhedral or polygonal shapes in the absence of fluids or melts in order to minimize grain surface energy (Etheridge, 1975; Altenberger, 1992; Suhr, 1993; Ross and Wilks, 1996). In the ultra high-temperature shear zone, orthopyroxene occurs as strain free, subhedral tablet grains with grain boundaries corresponding to crystallographic directions. The subhedral tablet orthopyroxene either crystallized directly from interstitial melts, or are the products of the recrystallization of primary orthopyroxene by melt- or fluid-assisted grain boundary migration (Drury and van Roermund, 1989). In Fig. 3(d), isolated subhedral orthopyroxene grains, which are aligned parallel to the shear foliation, are also completely enclosed within a single plagioclase grain. They do not replace primary orthopyroxene porphyroclasts, consequently they must have crystallized and grown from interstitial melts. Large orthopyroxene grains, which are elongate parallel to the foliation, are also strain free, suggesting that they are the products of crystallization from interstitial melts rather than primary orthopyroxenes which have been deformed and flattened parallel to the foliation. Based on the microstructures, the orthopyroxene petrofabrics are therefore interpreted as products of crystallization and oriented growth parallel to the shear foliation.

In the absence of pigeonite, the maximum temperature recorded by the assemblage orthopyroxene–olivine–clinopyroxene is 940°C, that is, 110°C below the solidus temperature of the anorthosite body. Upon cooling, pigeonite, a Ca-poor clinopyroxene, inverts to orthopyroxene with exsolutions of clinopyroxene. Inverted pigeonite in the shear zone may have recrystallized to orthopyroxene and clinopyroxene as deformation progressed to temperatures below the solidus temperature of the intrusion. Alternatively, the growth of clinopyroxene grains from exsolutions may simply be due to solid-state readjustment of high-angle boundaries to minimize surface energy. The temperatures recorded by the assemblage orthopyroxene–olivine–clinopyroxene are therefore only minimum temperatures for the deformation.

In summary, the dissected grain microstructures in plagioclase, the plagioclase petrofabrics, the near absence of deformation microstructures in both plagioclase and orthopyroxene, and the tablet crystal habit of orthopyroxene are collectively indicative of deformation and recrystallization at very high temperatures with melt present. Orthopyroxene petrofabrics can be interpreted either in terms of oriented growth or plastic deformation, but the microstructures suggest that they result from the crystallization and growth of orthopyroxene parallel to the shear foliation.

Microstructures in the subsolidus shear zone are very different from those in the ultra high-temperature shear zone. The shear zones initiated as fractures and faults, which evolved into narrow shear zones by recrystallization of plagioclase, orthopyroxene and olivine into small polygonal grains. Recrystallization of plagioclase and othopyroxene occurred by grain boundary rotation recrystallization, corresponding to Regime 2 creep of Hirth and Tullis (1992). The grains subsequently adjusted their grain boundary to minimize surface area and energy. No melt or fluid was present during deformation.

Fracturing was the first step in the formation of the subsolidus shear zone in the Poe Mountain anorthosite. Microfracturing and rotation recrystallization of plagioclase along fractures is common in granulite-facies shear zones, where large elongate plagioclase porphyroclasts are surrounded by small polygonal recrystallized grains (Ji and Mainprice, 1990). The transition from early cataclastic flow to plastic flow in feldspar aggregates has also been experimentally investigated by Tullis and Yund (1985, 1987); therefore, fracturing may be an important early process in the formation of subsolidus shear zones in all mafic rocks.

Plagioclase microstructures in the ultra high-temperature and subsolidus shear zones resemble asthenospheric and lithospheric olivine microstructures in ophiolites (Nicolas, 1986; Ceuleneer *et al*., 1988; Suhr, 1993). Asthenospheric microstructures are characterized by coarse olivine with strong CPO and flat extinction, similar to plagioclase microstructures in the ultra high-temperature shear zone, whereas lithospheric lower temperature microstructures are characterized by deformed fine-grained olivine neoblasts surrounding strongly deformed porphyroclasts (subsolidus shear zone).

CONCLUSIONS

To conclude, the following microstructural criteria can be used for differentiating ultra high-temperature shear zones from subsolidus granulite-facies shear zones in mafic rocks.

Ultra high-temperature shear zones

1. Shear zones are characterized by coarse plagioclase with flat extinction and few deformation microstructures.
2. Plagioclase has dissected grain microstructures, indicating recrystallization by 'fast' grain boundary migration (Regime 3 creep of Hirth and Tullis, 1992).
3. Orthopyroxene crystallized and grew into strain-free, tablet grains, which are elongate parallel to the shear foliation.
4. Plagioclase petrofabrics have poles to (010) normal to the shear foliation, and [100] parallel to the foliation and movement direction. Poles to (001) have a diffuse point distribution with a maximum concentration lying within the shear foliation and roughly normal to the movement direction.

Subsolidus granulite-facies shear zones

1. Shear zones consist of strongly strained primary minerals surrounded by smaller recrystallized grains.
2. Intragranular recrystallized fractures cut across primary plagioclase. Subsolidus shear zones may have initiated as fractures, which evolved into wider ductile shear zones with dynamic recrystallization.
3. Plagioclase and orthopyroxene recrystallized by grain boundary rotation recrystallization into small polygonal grains (Regime 2 creep of Hirth and Tullis, 1992).
4. Plastic deformation of plagioclase produces two types of petrofabrics, as reported in the literature. At amphibolite- to granulite-grade temperatures, (010) is parallel to the shear foliation, [001] is parallel to the movement direction, and [100] is perpendicular to both shear foliation and movement direction. At higher temperatures and/or An content in plagioclase, (001) is parallel to the shear foliation, [100] is parallel to the movement direction, and [010] is perpendicular to both shear foliation and movement direction.

Acknowledgements—We thank James Scoates for helpful discussions, and Susan Swapp for assistance with the microprobe analyses. Keith Benn and an anonymous reviewer are thanked for their reviews, and J. C. White for his editorial comments.

REFERENCES

Altenberger, U. (1992) Stress-induced natural transformation of ortho- to clinohypersthene in metagabbros of the Ivrea Zone, Northern Italy. *Mineralogy and Petrology* **46,** 43–48.

Anderson, D. J., Lindsley, D. H. and Davidson, P. M. (1993) QUILF: A Pascal program to assess equilibria among Fe–Mg–Mn–Ti oxides, pyroxenes, olivine, and quartz. *Computers and Geosciences* **19,** 1333–1350.

Ballhaus, C. and Berry, R. F. (1991) Crystallization history of the Giles Layered Igneous Complex, central Australia. *Journal of Petrology* **32,** 1–28.

Benn, K. and Allard, B. (1989) Preferred mineral orientations related to magmatic flow in ophiolite layered gabbros. *Journal of Petrology* **30,** 925–946.

Benn, K. and Mainprice, D. (1989) An interactive program for determination of plagioclase crystal axes orientations from U-stage measurements: an aid for petrofabric studies. *Computers and Geosciences* **15,** 1127–1142.

Boullier, A. M. and Nicolas, A. (1975) Classification of textures and fabrics of peridotite xenoliths from South African kimberlites. *Physics and Chemistry of the Earth* **9,** 467–475.

Carter, N. L. and Raleigh, C. B. (1969) Principal stress directions from plastic flow in crystals. *Geological Society of America Bulletin* **80,** 1231–1264.

Ceuleneer, G., Nicolas, A. and Boudier, F. (1988) Mantle flow patterns at an oceanic spreading center: the Oman peridotites record. *Tectonophysics* **151,** 1–26.

Christensen, N. I. and Lundquist, S. M. (1982) Pyroxene orientation within the upper mantle. *Geological Society of America Bulletin* **93,** 279–288.

Drury, M. R. and van Roermund, H. L. M. (1989) Fluid assisted recrystallization in Upper mantle peridotite xenoliths from kimberlites. *Journal of Petrology* **30,** 133–152.

Etheridge, M. A. (1975) Deformation and recrystallization of orthopyroxene from the Giles Complex, central Australia. *Tectonophysics* **25,** 87–114.

Frost, B. R., Frost, C. D., Lindsley, D. H., Scoates, J. S. and Mitchell, J. N. (1993) The Laramie Anorthosite Complex and Sherman batholith: geology, evolution, and theories of origin. In *Geology of Wyoming*, ed. A. W. Snoke, J. R. Steidtmann and S. M. Roberts, pp. 118–161. Geological Survey of Wyoming Memoir **5**.

Fuhrman, M. L., Frost, B. R. and Lindsley, D. H. (1988) Crystallization conditions of the Sybille monzosyenite, Laramie anorthosite complex, Wyoming. *Journal of Petrology* **29,** 699–729.

Grant, J. A. and Frost, B. R. (1990) Contact metamorphism and partial melting of pelitic rocks in the aureole of the Laramie anorthosite complex, Morton Pass, Wyoming. *American Journal of Science* **290,** 425–472.

Hirth, G. and Tullis, J. (1992) Dislocation creep regimes in quartz aggregates. *Journal of Structural Geology* **14,** 145–159.

Ji, S. and Mainprice, D. (1988) Natural deformation fabrics of plagioclase: implications for slip systems and seismic anisotropy. *Tectonophysics* **147,** 145–163.

Ji, S. and Mainprice, D. (1990) Recrystallization and fabric development in plagioclase. *Journal of Geology* **98,** 65–79.

Ji, S., Zhao, X. and Zhao, P. (1994) On the measurement of plagioclase lattice preferred orientations. *Journal of Structural Geology* **16,** 1711–1718.

John, B. E. and Blundy, J. D. (1993) Emplacement-related deformation of granitoid magmas, southern Adamello Massif, Italy. *Geological Society of America Bulletin* **105,** 1517–1541.

Kelemen, P. B. and Dick, H. J. B. (1995) Focused melt flow and localized deformation in the upper mantle: Juxtaposition of replacive dunite and ductile shear zones in the Josephine peridotite, SW Oregon. *Journal of Geophysical Research* **100,** 423–438.

Kruhl, J. H. (1987) Preferred lattice orientations of plagioclase from amphibolite and greenschist facies rocks near the Insubric Line (Western Alps). *Tectonophysics* **135,** 233–242.

Lafrance, B., John, B. E. and Scoates, J. S. (1996) Syn-emplacement recrystallization and deformation microstructures in the Poe Mountain anorthosite, Wyoming. *Contributions to Mineralogy and Petrology* **122,** 431–440.

Mainprice, D. and Silver, P. G. (1993) Interpretation of SKS-waves using samples from the subcontinental lithosphere. *Physics of the Earth and Planetary Interiors* **78,** 257–280.

Means, W. D. (1983) Microstructure and micromotion in recrystallization flow of octachloropropane: a first look. *Geologische Rundschau* **72,** 511–528.

Moore, A. C. (1973) Studies of igneous and tectonic textures and layering in the rocks of the Gosse pile intrusion, central Australia. *Journal of Petrology* **14,** 49–79.

Nicolas, A. (1986) Structure and petrology of peridotites: clues to their geodynamic environment. *Reviews in Geophysics* **24,** 875–895.

Nicolas, A., Boudier, F. and Boullier, A. M. (1973) Mechanisms of flow in naturally and experimentally deformed peridotites. *American Journal of Science* **273,** 853–876.

Olesen, N. Ø (1987) Plagioclase fabric development in a high-grade shear zone, Jotunheimen, Norway. *Tectonophysics* **142,** 291–308.

Olsen, T. S. and Kohlstedt, D. L. (1985) Natural deformation and recrystallization of some intermediate plagioclase feldspars. *Tectonophysics* **111,** 107–131.

Park, Y. and Means, W. D. (1996) Direct observation of deformation processes in crystal mushes. *Journal of Structural Geology* **18,** 847–858.

Raleigh, C. B., Kirby, S. H., Carter, N. L. and Ave'Lallemant, H. G. (1971) Slip and the clinoenstatite transformation as competing rate processing in enstatite. *Journal of Geophysical Research* **76,** 4011–4022.

Ross, J. V. and Wilks, K. R. (1996) Microstructure development in an experimentally sheared orthopyroxene granulite. *Tectonophysics* **256,** 83–100.

Schmidt, E. R. (1952) The structure and composition of the Merensky Reef and associated rocks on the Rustenberg platinum mine. *Transactions of the Geological Society of South Africa* **55,** 233–279.

Scoates, J. S. (1994) Magmatic evolution of anorthositic and monzonitic rocks in the mid-Proterozoic Laramie anorthosite complex, Wyoming, U.S.A. Ph.D. dissertation, University of Wyoming, Laramie.

Skrotzki, W., Wedel, A., Weber, K. and Müller, W. F. (1990) Microstructure and texture in lherzolites of the Balmuccia massif and their significance regarding the thermomechanical history. *Tectonophysics* **179,** 227–251.

Suhr, G. (1993) Evaluation of upper mantle microstructures in the Table Mountain massif (Bay of Islands ophiolite). *Journal of Structural Geology* **15,** 1273–1292.

Tobisch, O. T., Renne, P. R. and Saleeby, J. B. (1993) Deformation resulting from regional extension during pluton ascent and emplacement, central Sierra Nevada, California. *Journal of Structural Geology* **15,** 629–646.

Tullis, J. and Yund, R. A. (1985) Dynamic recrystallization of feldspar: a mechanism for ductile shear zone formation. *Geology* **13,** 238–241.

Tullis, J. and Yund, R. A. (1987) Transition from cataclastic flow to dislocation creep of feldspar: mechanisms and microstructures. *Geology* **15,** 606–609.

Tungatt, P. D. and Humphreys, F. J. (1984) The plastic deformation and dynamic recrystallization of polycrystalline sodium nitrate. *Acta Metallurgica* **32,** 1625–1635.

Urai, J. L. (1983) Water assisted dynamic recrystallization and weakening in polycrystalline bischofite. *Tectonophysics* **96,** 125–157.

Urai, J. L., Means, W. D. and Lister, G. S. (1986) Dynamic recrystallization of minerals. In *Mineral and Rock Deformation: Laboratories Studies. The Paterson Volume*, ed. B. E. Hobbs and H. C. Heard, pp. 161–199. American Geophysical Union Geophysical Monograph **36**.

Vernon, R. H., Paterson, S. R. and Geary, E. E. (1989) Evidence for syntectonic intrusion of plutons in the Bear Mountain fault zone, California. *Geology* **17,** 723–726.

Zhao, X-O., Ji, S. and Martignole, J. (1995) Plastic deformation and crystallographic orientations of plagioclase in the high-grade Morin Terrane (Grenville Province), Québec [abstract]. In *Canadian Tectonic Group '95 Annual Meeting, Rawdon, Québec.*